

INVESTIGATION OF DIFFERENTIAL SURFACE REMOVAL DUE TO ELECTROPOLISHING AT JLAB*

F. Marhauser[#], J. Follkie, C.E. Reece, Jefferson Laboratory, Newport News, VA, USA

Abstract

The surface removal of JLab's present electropolishing process has been analyzed utilizing experimental data of six nine-cell 1.3 GHz superconducting radio frequency cavities that have been chemically post-processed in the frame of the LCLS-II high-Q development plan.

INRODUCTION

Surface chemistry carried out for superconducting radio frequency (SRF) cavities such as buffered chemical polishing (BCP) and electropolishing (EP) aims to uniformly remove the interior surface of a cavity along the entire structure and within each cell from equator to iris. A uniform removal is not readily achievable for either BCP or EP - though conceptually different - due to the complex chemical processes and varying process parameters (e.g. fluid flow, temperatures). The process-specific differential surface removal for instance impacts the cavity cell target frequency defined at the manufacturing stage. Quantifying the non-uniform removal helps to concurrently obtain the desired frequency and field flatness of an SRF cavity with minimum tuning effort and within tight tolerances [1]. An assessment of JLab's BCP system has been done in the past. The differential surface removal as experienced in the EP system has been quantified more recently as described in the following. It is based on experimental data in conjunction with numerical simulations. This includes the impact of EP on a cavity's fundamental mode field flatness.

MEASURMENTS

Removal from Integrated Current

Six LCLS-II (TESLA-type) R&D cavities (AES031-036) have been processed in the frame of the high-Q development plan [2]. The cavities have received a main (bulk) EP in preparation of the Nitrogen-doping, which is carried out as part of the 800°C vacuum furnace bake-out. A final (light) EP is applied after the doping process. The rather slow EP generally polishes the interior with a mixture of hydrofluoric acid and concentrated sulfuric acid. The EP at JLab is carried out horizontally (see Fig. 1). To stabilize process temperatures along the cavity, the external surface is constantly water-cooled via spray nozzles from below the cavity, while the cavity rotates (1 rpm). Cavity wall temperatures can typically be controlled within 20-25°C. To estimate the removal during the EP process, the accumulated charge is

determined by recording the current over time flowing from the inserted cathode to the anode (cavity) taking into account the surface area of the cavity. With five electrons per niobium atom removed from anode and cathode reactions, the bulk removal rate is $2.247e-5 \text{ cm}^3 \text{ Nb/Cb}$. The nominal voltage between cathode and anode is $13.5 \pm 0.2 \text{ V}$. The EP process is stopped once the prospected removal is achieved. The assessed wall removal based on this method is summarized in Table 1. The main rather slow EP was carried out in two steps for operational convenience since the duration consumes more than a normal workday. The total removal by EP was around $140 \mu\text{m}$ at this point of time and well controlled among cavities.



Figure 1: Left: LCLS-II R&D cavity prepared for EP at JLab. Right: Arrangement of water-spray nozzles for external cooling of cavity walls.

Table 1: Wall Removal Evaluated from the Integrated Current for the Main (1st And 2nd Pass) and Final EP

Cavity ID	Main EP 1 st pass (μm)	Main EP 2 nd pass (μm)	Final EP (μm)	Total (μm)
AES-031	106.9	21.4	16.1	144.4
AES-032	96.2	26.7	16.1	139.0
AES-033	96.2	26.7	16.0	139.0
AES-034	96.2	26.7	16.1	139.0
AES-035	90.9	32.1	16.1	139.0
AES-036	96.2	26.7	16.1	139.0

Ultra-sonic Thickness Measurements

Though the assessment based on the integrated current is sufficiently accurate to control the EP process, it does not provide information with regard to the differential removal between irises and equators. Therefore, wall thickness measurements utilizing an ultra-sonic (US) gauge have been performed before and after the main EP. The measurements include one location close to the equator and one close the stiffening ring for each half cell. Locations below stiffening rings and close to irises are not accessible. Yet, measurements have been done directly on the beam tubes adjacent to end cells. Figure 2 plots the removal averaged for four repetitive measurements per location along each cavity to consider systematic errors. A quite uniform removal among equators has been

* Authored by Jefferson Science Associates, LLC under U.S. DOE Contract No. DE-AC05-06OR23177
[#] marhause@jlab.org

achieved throughout. The averaged data reveal a consistently larger removal closer to the stiffening rings than within the equator dome region. Deviations range from 2 μm (AES-034, AES-035) to 16 μm (AES-031, AES-036). The removal in the beam tubes is typically more than twice the removal in the equator dome region. This also implies a significant differential polishing between equators and irises, although the interior irises were water cooled, but the cavity end-groups in the beam tubes not. Moreover, Fig. 2 reveals a bias, i.e. a smaller removal on one side (fundamental power coupler (FPC) port side) than on the other side of the cavity. The latter corresponds to the right side in Fig. 1. Here the beam tube was not readily accessible for water spraying from the bottom.

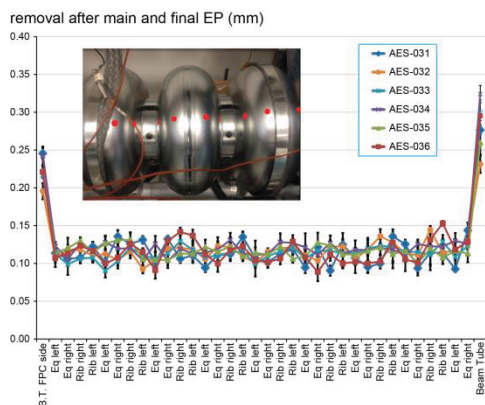


Figure 2: Total wall removal (after main and final EP) as measured with a US gauge along each cavity as denoted in the legend. The embedded photo illustrates where measurements were taken (red dots) for inner cells.

Table 2 summarizes the measured average data differentiating between locations close to equators, stiffeners and on beam tubes, respectively. The values are in reasonable agreement with the removal assessed theoretically in Table 1 after the main EP, but reveal the differential removal between the two locations.

Table 2: Averaged Wall Removal from US Thickness Measurements after the Main EP

Cavity ID	Close to equators (μm)	Close to stiffeners (μm)	Beam tubes avg. (left/right) (μm)
AES-031	110	116	261 (246/277)
AES-032	112	120	213 (196/231)
AES-033	109	117	258 (216/300)
AES-034	118	120	283 (242/342)
AES-035	115	117	241 (222/260)
AES-036	107	123	258 (221/295)

The observed variations among cavities seem to be linked to process temperatures as recorded during the main EP. For instance, Table 3 denotes the difference of average wall temperatures ($\langle\Delta T\rangle = \langle T_{\text{tubes}} \rangle - \langle T_{\text{cells}} \rangle$) between beam tubes (both sides) and cavity cells (recorded at cells 1, 3, 5, 7 and 9). This temperature

difference is relatively small for AES-032 and AES-035, which also exhibited the least amount of beam tube wall removal as listed in Table 2. The maximum temperature difference ($\Delta T_{\text{max}}(t_i)$) observed between beam tubes and cells covering the entire process time (evaluated at time stamps (t_i) 30 min apart) on the other hand is significantly larger than $\langle\Delta T\rangle$ and exceeded 10°C for AES-031 and AES-036 at a few times during the process. The water temperature was typically kept below 20°C for less aggressive polishing, but cannot be well controlled at present, such that the water spray temperature varied during the EP process, which in turn can influence the polishing rate.

Table 3: Average and Maximum Wall Temperature Differences Measured between Tubes and Cavity Cells

Cavity ID	Main EP (1 st pass)	Main EP (2 nd pass)	Main EP (1 st pass)	Main EP (2 nd pass)
	$\langle\Delta T\rangle$ ($^\circ\text{C}$)		$\Delta T_{\text{max}}(t_i)$ ($^\circ\text{C}$)	
AES-031	5.4	4.9	11.5	7.8
AES-032	3.6	2.2	8.4	5.8
AES-033	5.1	5.3	9.9	9.9
AES-034	4.3	4.0	7.0	6.8
AES-035	3.1	2.2	6.4	4.2
AES-036	6.6	5.8	12.5	10.6

NUMERICAL SIMULATIONS

Removal Implied by Frequency Change

The frequency reduction due to EP is another way to obtain more insights into the actual differential surface removal when supported by numerical calculations. A relatively large frequency change (per given equator removal) indicates a more uniform removal process. This is due to the fact that the frequency decreases when the wall material is removed at the equator (magnetic field increase dominant), while it increases when wall material is removed at the iris (electric field decrease dominant). Table 4 lists the frequency removal rate assessed for each cavity and normalized to the measured removal at equators. The average value of this rate combining all cavities is $-5.25 \text{ kHz}/\mu\text{m}$. AES-035 exhibits the maximum value, which implies the most uniform removal, while the least uniform removal is observed for AES031. As listed in Table 2, in fact a comparably small difference in the absolute removal between equator and stiffening ring locations has been observed for AES035 (2 μm) as compared to AES031 (16 μm).

Table 4: Frequency Change (Δf) Due to EP and Corresponding Removal Rate in $\text{kHz}/\mu\text{m}$ Referred to the Equator

Cavity ID	Δf after main EP (MHz)	Δf per removal at equator ($\text{kHz}/\mu\text{m}$)
AES-031	-0.465	-4.23
AES-032	-0.627	-5.58
AES-033	-0.555	-5.07
AES-034	-0.548	-4.66
AES-035	-0.783	-6.80
AES-036	-0.548	-5.14

The removal rate serves well to quantify the differential etching. It can be conceived that the differential polishing evolves smoothly from iris to equator rather than abruptly. To resemble this situation we assumed that the equator ellipse half axes forming a cell increase in horizontal and vertical direction, whereas the iris ellipse half axes decrease by a larger amount concurrently. For the simulations an equator removal of 115 μm has been chosen as reference, which corresponds to about the bulk EP removal amount measured. The iris half axes have then been varied such to study different equator-to-iris removal ratios covering 0.55 to 1 (uniform removal). Since the removal rate for a nine-cell cavity is close to that of a single mid-cell, only the mid-cell has been modelled to simplify the calculations. The results are plotted in Fig. 3. For an average removal rate of $-5.25 \text{ kHz}/\mu\text{m}$, the finding implies that the ratio is ~ 0.58 .

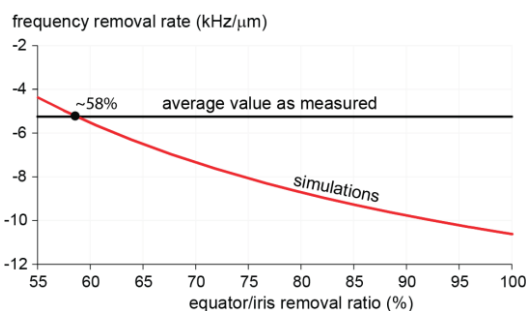


Figure 3: Frequency removal rate versus removal ratio of equator to iris.

In the same manner, the iris removal can be independently assessed for each cavity based on the individual removal rates combined with US gauge measurements as listed in Table 2. Note that the surface removal at the beam tubes has been found much higher than the estimated removal at cavity irises (see Table 5). This can be attributed to the higher wall and thus process temperatures within the beam tubes.

Table 5: Estimated removal at irises after main EP

Cavity ID	Equator/iris removal ratio (%)	Estimated removal at irises (μm)
AES-031	54.3	202.3
AES-032	60.0	187.4
AES-033	57.8	189.2
AES-034	56.1	209.4
AES-035	65.0	177.2
AES-036	58.1	183.3

Impact on Field-Flatness

To numerically quantify the impact of the non-uniform EP on the field profile, a bare nine-cell LCLS-II cavity has been modeled. The model allows differentiating between mid-cells and end cups (plus beam tubes). The cavity has been tuned field flat numerically – is not flat by design – by adjusting end cell equators (radial tuning).

Exemplarily, Fig. 4 shows the on-axis electrical RF field profile measured (left) and calculated numerically (right) for AES032 resembling the conditions before/after the main EP (red/green curves). The differential surface removal at end cups has been taken into account in conjunction with the differing beam tube removal on each cavity side as observed experimentally. This produces a field asymmetry after EP with respect to the cavity center seen in both the measurement and the simulation. A reduction of field amplitudes in end cells in the order of 5-10% has been observed after the main EP. The measured reduction is well resembled numerically in the cell adjacent to the FPC port (short end cup side). The largest field amplitude reduction is observed on the long end cup side for both cases, but more pronounced in the measurements. However, a biased field was already present prior to the EP due to insufficient tuning, which might explain the main discrepancy between experiment and simulation. A large uncertainty still relates to the rather unknown polishing amount within the cells closest to the beam tubes, which can have a significant impact on the field profile.

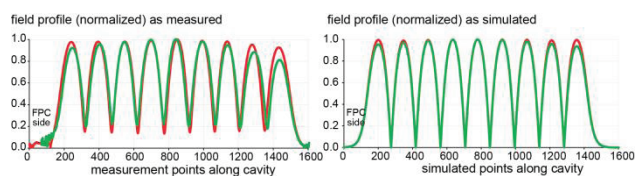


Figure 4: Electrical field profile for the TM_{010} π -mode as measured (left) and resembled numerically (right) for AES032 before (red) and after (green) main EP.

The frequency change measured for AES-032 due to the non-uniform main EP was -627 kHz (see Table 4) with unknown ambient conditions and hence a few ten kHz uncertainty. The simulation resulted in -663 kHz and is thus in well agreement with the experimental finding.

SUMMARY

In pursuit of a better understanding of the differential polishing of cavities in JLab's EP facility, experimental data have been analyzed in combination with numerical calculations. This revealed that the equator-to-iris removal ratio is in the order of 60%. The impact on the field flatness after EP has been quantified. Based on the results it is suggested to pre-tune cavities in a way to leave higher peak amplitudes in end cells such that a flatter field can be achieved after the main EP. This will minimize bench tuning effort and thus cavity cell distortions and is beneficial to expedite the post-processing procedures.

REFERENCES

- [1] F. Marhauser, JLab-TN-10-021, August 2010.
- [2] C. Reece, JLab-TN-14-015, July 2014.